

# A Novel Avenue to Gold Nanostructured Microtubes Using Functionalized Fiber as the Ligand, the Reductant, and the Template

Hongjuan Ma,<sup>†,‡</sup> Hongying Chi,<sup>†,§</sup> Jingxia Wu,<sup>†,§</sup> Min Wang,<sup>†</sup> Jingye Li,<sup>\*,†</sup> Hiroyuki Hoshina,<sup>‡</sup> Seiichi Saiki,<sup>‡</sup> and Noriaki Seko<sup>‡</sup>

<sup>†</sup>TMSR Research Center and CAS Key Lab of Nuclear Radiation and Nuclear Energy Technology, Shanghai Institute of Applied Physics, Chinese Academy of Sciences, Shanghai 201800, P. R. China

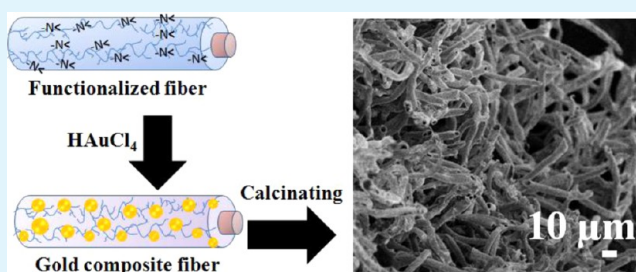
<sup>‡</sup>Quantum Beam Science Directorate, Japan Atomic Energy Agency, 1233 Watanuki, Takasaki, Gunma 370-1292, Japan

<sup>§</sup>University of the Chinese Academy of Sciences, Beijing 100049, P. R. China

## S Supporting Information

**ABSTRACT:** Gold nanostructured microtubes (AuNMTs) are prepared using a tertiary amine group-functionalized polyethylene (PE)-coated polypropylene (PP) nonwoven fabric as a ligand, a reductant, and a template, which takes advantage of the different radiation effects of PE and PP. The Au(III) ions are absorbed and reduced only in the PE layer to form the aggregation of gold nanoparticles; thus, AuNMTs are obtained after the calcination.

**KEYWORDS:** gold nanostructured microtubes, radiation-induced graft polymerization, ligand, reductant, template



## INTRODUCTION

Noble metal nanostructures, especially gold nanostructures, have a rich history in both synthesis and application<sup>1</sup> because of their fascinating size-dependent properties and important applications in catalysis,<sup>2,3</sup> surface-enhanced Raman scattering (SERS),<sup>4</sup> sensing,<sup>5,6</sup> separation,<sup>7,8</sup> optoelectronics,<sup>9</sup> optics,<sup>10</sup> and information storage.<sup>11</sup> For example, biomedical applications of gold nanoparticles (AuNPs) started in 1971 with the use of an antibody–AuNP complex for cell surface antigen localization.<sup>12</sup> In the field of heterogeneous catalysis, researchers reported an exciting discovery with the observation that nanoparticles of gold on a large surface area support a high activity for oxidation of CO with O<sub>2</sub> at room temperature.<sup>3</sup> Initially, microscopic materials with solid structures of gold particles or spheres attracted tremendous interest because of the thermodynamically and kinetically favorable morphology of particles or spheres. In the same era, to weaken the propensity for isotropic growth and direct the growth of the nanoparticle into an anisotropic dimension, trilateral nanoplates were created and soon set off a new upsurge in nanogold.<sup>13</sup> A few years ago, single crystalline nanoboxes of gold with a hollow polyhedron bounded by six (100) and eight (111) facets were generated.<sup>14</sup> Recently, another class of gold nanorods with an anisotropic structure has received a great deal attention because of their unique optical and electronic properties that are dependent on their shape, size, and aspect ratio.<sup>15</sup>

Tubular nanostructure has become a hot research topic since the first report of carbon nanotubes by Iijima in 1991,<sup>16</sup> which was followed by many reports on the nanotubes of metal,<sup>17</sup> metal oxide,<sup>18</sup> and various composites.<sup>19,20</sup> Gold nanotubes

(AuNTs) made from a template of silica,<sup>21</sup> alumina,<sup>22</sup> silicon, and other metals<sup>23</sup> were also developed. In the 1990s, Martin and co-workers reported the synthesis of AuNTs by electrochemically depositing gold into the pores of microporous alumina.<sup>24</sup> AuNTs have also been prepared by deposition in the pores of track-etched polycarbonate membranes that contain 10 μm thick and 220 nm diameter pores.<sup>3,25,26</sup> Goethite nanorods have been used as templates to grow gold nanotubes with a length of a few hundred nanometers and an aspect ratio between 3 and 4.<sup>27</sup> In general, the diameters of the obtained AuNTs and AuNMTs in the literature range from tens to hundreds of nanometers, and some of the AuNTs could be made as small as several nanometers.<sup>28</sup>

Almost all procedures for the preparation of AuNTs and AuNMTs involve a template, which is probably the most familiar means of synthesis with good reliability and control. There are variant classifications of templates either by the physicochemical property or by the morphology of the materials used. With respect to physicochemical properties and the removal method, templates can be divided into two types. Hard templates such as aluminum oxide and silver can be removed by chemical etching;<sup>29,30</sup> soft templates such as solid-state polymers and liquid-state crystals or gels can be removed by calcinations,<sup>31</sup> plasma etching, or dissolution of the polymer in an appropriate solvent.<sup>32</sup> Without removal of the templates, some composite nano-microstructured fibers were also

Received: July 2, 2013

Accepted: August 9, 2013

Published: August 9, 2013

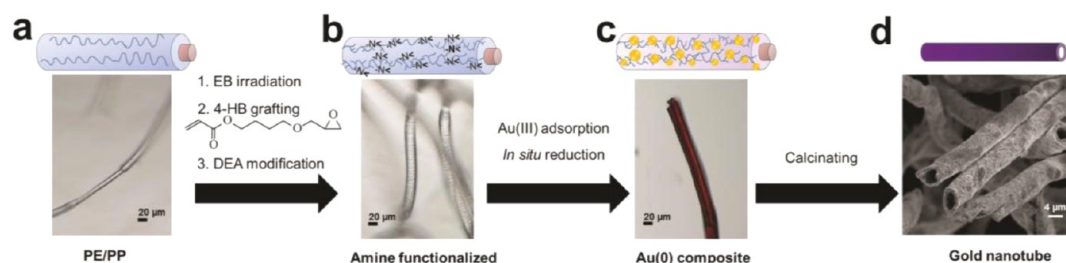


**Figure 1.** Fabrication of AuNMTs: (a) PE/PP nonwoven fabric and its microscopy image, (b) tertiary amine group-functionalized PE/PP fabric and its microscopy image, (c) gold absorbed and reduced fiber and its microscopy image, and (d) AuNMTs and their scanning electron microscopy image.

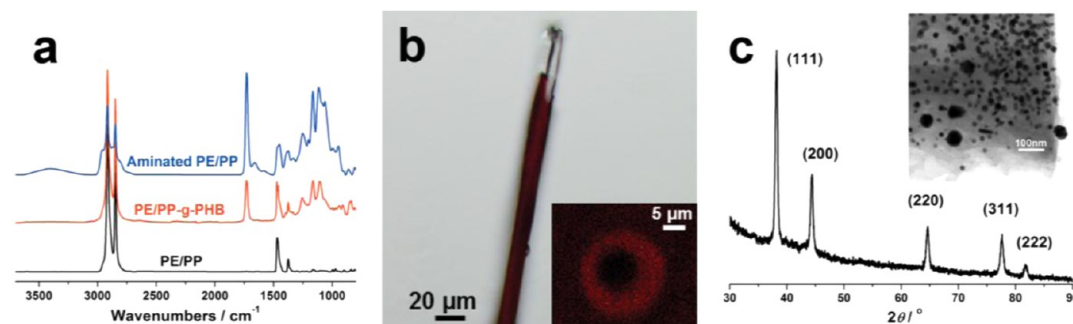


**Figure 2.** (a) FT-IR spectra of pristine PE/PP nonwoven fabric, PE/PP-g-PHB fabric, and tertiary amine group-functionalized PE/PP fabric. (b) Microscopy image of the core-shell structure of the gold absorbed and reduced fiber. The inset shows the scanning electron microscopy image of the cross section of the gold absorbed and reduced fiber. (c) XRD pattern of the absorbed and reduced gold nanoparticles on the fabric. The inset shows the TEM image of gold nanoparticles loaded in the fiber.

obtained.<sup>33,34</sup> At the beginning of the AuNT study, researchers came across one critical problem in large-scale production and application, which is the difficulty in the preparation of the template and the subsequent coating process. After a long period, with the development of a new method and technology, a great step forward in the fabrication of nanotubes was taken. Electrospun fiber mats,<sup>32</sup> electroless plating, and commercial polymer fibers<sup>33,34</sup> were used, nanoscale metallization processes that can easily be scaled. In this study, we report a novel avenue for producing AuNMTs based on a multifunctional soft template that also plays a role as a ligand and a reductant, which is made from industrially available polyethylene-coated polypropylene (PE/PP) nonwoven fabric (Figure S1 of the Supporting Information). The multifunctional soft template preparation takes advantage of the different radiation effects of the shell PE layer and core PP layer of the fiber (Figure 1a), where the monomer, 4-hydroxybutyl acrylate glycidylether (HB), is only graft polymerized onto the shell PE layer and, therefore, the tertiary amino groups exist only in the shell layer that reacted with the epoxy groups on the graft chains (Figure 1b). Hence, the Au(III) ions are adsorbed by the tertiary amino groups as the ligands and then *in situ* reduced, forming AuNPs deposited in the shell layer (Figure 1c). Finally, the template is removed by calcination and AuNMTs are obtained (Figure 1d).

## EXPERIMENTAL SECTION

**Materials.** Polyethylene-coated polypropylene (PE/PP) nonwoven fabric was obtained from Kurashiki MFG Co. 4-Hydroxybutyl acrylate glycidylether (HB) was purchased from Tokyo Kasei Kogyo Co. Ltd. and used without further purification. Diethylamine (DEA), surfactant sorbitan monolaurate (Span-20), and isopropyl alcohol (IPA) were purchased from Kanto Chemical Co. Ltd. Analytical-grade HAuCl<sub>4</sub>·4H<sub>2</sub>O was used to prepare Au(III) solutions.

**Preparation.** PE/PP nonwoven fabric samples were irradiated with an absorbed dose of 30 kGy by electron beam (EB). The irradiated samples were put into a glass ampule, and the ampule was evacuated. Then an emulsion containing 5% HB and 0.5% surfactant Span-20 was drawn into the glass ampule via suction. The graft polymerization was conducted at 40 °C for 2 h, and then the grafted samples were taken out and washed with methanol to remove any residue homopolymers and then dried in vacuum. The degree of grafting (DG) of the obtained PE/PP-g-PHB was 150%, which was determined by calculating the weight increment ratio. The grafted materials were immersed in a 50% DEA/water solution at 30 °C for 5 h, removed, washed with distilled water, and finally dried in vacuum. As a result, the tertiary amine group-functionalized PE/PP nonwoven fabrics were obtained.

The functionalized PE/PP fabrics were soaked in a chloroauric acid solution with a specific Au(III) concentration varying from 1 to 100 ppm. After reacting for 2 h, the samples were taken out and washed. The AuNMTs were obtained by calcination, which was conducted in an electric muffle furnace in the presence of O<sub>2</sub> to 800 °C at a heating rate of 10 °C/min.

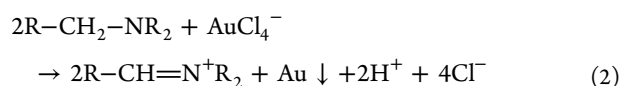
**Characterization.** The morphology of the nonwoven fabric under low magnification was observed with a microscope (Olympus BX53). The surface and cross section of the nonwoven fabric were observed with a scanning electron microscope (Hitachi SEM-EDX Type-N), after the adsorbent had been dried under reduced pressure and gold coating for 120 s. The distribution of metal ion across the adsorbent was determined by means of an electron probe X-ray microanalyzer (XMA). The surface and cross section of AuNMTs were observed with a scanning electron microscope (Hitachi S-4800). The morphology of gold particles was observed by transmission electron microscopy (TEM) (FEI TECNAI G2) and X-ray diffraction (XRD).

## RESULTS AND DISCUSSION

PE and PP are very similar in chemical structure; however, the radicals generated in PE are relatively stable, which can induce graft polymerization or cross-linking, while the radicals

generated in PP always result in chain scission.<sup>35</sup> The graft polymerization of vinyl monomers initiated by the radicals in the fabrics is a mature procedure that has been used for several decades.<sup>36–38</sup> Success in the graft polymerization of HB and the following amination can be confirmed by a Fourier transform infrared (FT-IR) spectroscopy study (Figure 2a). Compared with the spectrum of the trunk PE/PP, the spectrum of the grafted materials (denoted as PE/PP-g-PHB) shows strong absorption bands at  $1726\text{ cm}^{-1}$ , which is attributed to C=O stretching, and  $1251\text{ cm}^{-1}$ , which is attributed to C–O stretching, together with  $910$  and  $842\text{ cm}^{-1}$  bands representing the characteristic vibrations of epoxy groups. The diameters of the fibers are changed by graft polymerization that is almost doubled to  $20\text{ }\mu\text{m}$  at a DG of 150% (Figure S2 of the Supporting Information). After the reaction of the epoxy groups with DEA, in the spectrum of the aminated PE/PP, the absorption bands attributed to characteristic vibrations of epoxy groups at  $910$  and  $842\text{ cm}^{-1}$  disappeared and a broad band at  $\sim 3400\text{ cm}^{-1}$  attributed to –OH stretching appeared. The characteristic peak at  $1200\text{ cm}^{-1}$  represents the C–N stretching vibration. The tertiary amine groups covalently bonded to the fabric are designed as the adsorbent for metal ions.<sup>39</sup> The fabric is dark violet after the adsorption of the Au(III) ion, which makes it easy to determine the core–shell structure (Figure 2b). The PP core layer is inert, while the PE shell layer is filled with gold; thus, a cylindrical “gold layer” with a wall thickness of around  $5\text{ }\mu\text{m}$  is formed and confirmed by SEM-EDX observation (inset of Figure 2b).

It is well-known that  $\text{AuCl}_4^-$  is a powerful oxidizing agent in aqueous solutions with standard reduction potentials ( $E^\circ$ ) of  $1.0\text{ V}$ .<sup>40</sup> It was reported that polymers with an amino group served as the reduction agent and stabilizer.<sup>40,41</sup> Therefore, the absorbed Au(III) ions are reduced in situ by means of the following equations.



The formation of metal gold after the reduction has been confirmed by XRD analysis, where it is a face-centered cubic (fcc) structure (JCPDS Card 04-0784) (Figure 2c), and the shape of the gold is a spherical nanoparticle with a diameter of approximately  $5\text{--}20\text{ nm}$  (inset of Figure 2c).

Finally, the polymer was removed by calcination, and the gold nanostructured microtubes were obtained. Scanning electron microscopy (SEM) images of the AuNMTs are presented in Figure 3a–d. Obviously, the wall thickness and the outer diameter are determined by the concentration of chloroauric acid used and are 1 order of magnitude lower than the thickness of the functionalized PE shell layer, which is  $\sim 5\text{ }\mu\text{m}$ , where the tertiary amino group density in the fabric is fixed. The rough wall morphology of the AuNMTs indicates that the AuNMTs are constructed from gold nanoparticles, which can be confirmed from the TEM image recorded from the edge of an individual tube (Figure S3 of the Supporting Information). The image shows that the gold nanoparticles exhibited an average diameter of  $5\text{--}20\text{ nm}$ , which is almost unchanged from that of the AuNMPs before calcination. The high-resolution TEM image (Figure S4 of the Supporting Information) shows (111) and (200) lattice fringes perpendicular to the tube axis with interplane spacing of  $\sim 0.23$  and  $\sim 0.20$

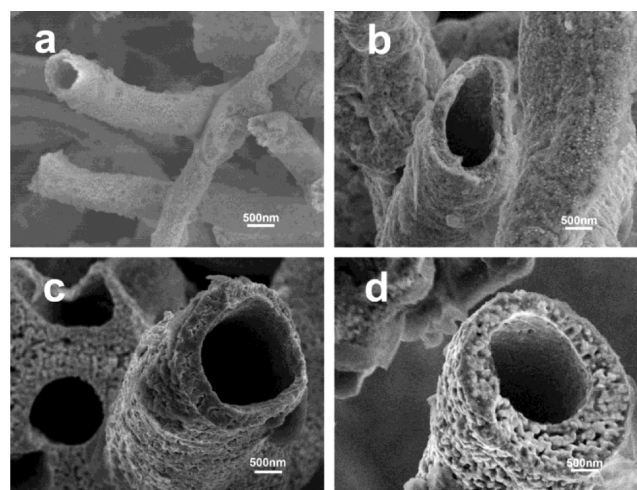


**Figure 3.** SEM images of AuNMTs prepared from the chloroauric acid solution with initial Au(III) concentrations of (a) 1, (b) 5, (c) 20, and (d) 60 ppm.

nm, respectively. The wall thickness of the AuNMTs and the diameter are determined by the Au(III) concentration and are presented in Figure 4, where the wall thickness and diameter

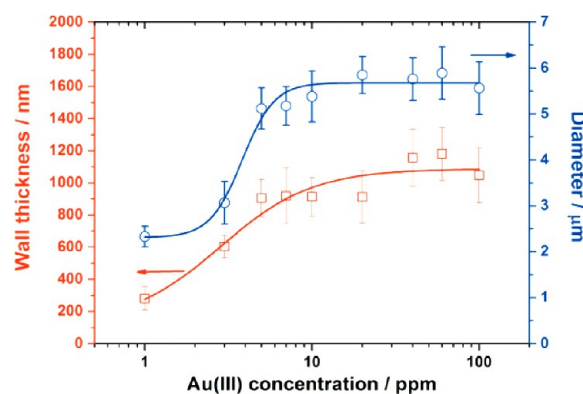


**Figure 4.** Dependence of the wall thickness and diameter of AuNMTs on the initial Au(III) concentration.

increase quickly with an increased Au(III) concentration and then leveled off. The shortest wall thickness and diameter obtained were  $280\text{ nm}$  and  $2.3\text{ }\mu\text{m}$ , respectively, with an initial Au(III) concentration of  $1\text{ ppm}$ . The saturated values for wall thickness and diameter were  $1000\text{ nm}$  and  $5.5\text{ }\mu\text{m}$ , respectively, when the initial Au(III) concentration was  $>7\text{ ppm}$ .

The length or slenderness ratio of the AuNMTs is an important parameter that is usually determined by the template used. Here, because we used a functionalized nonwoven fabric as the template, the obtained AuNMTs are also in a network form (Figure 5). The image shows the length of the AuNMTs between the junctions is  $\sim 200\text{ }\mu\text{m}$ , which demonstrated the advantage of using fiber or fabric as the template as compared to using porous films or inorganic nanorods as templates. If a long single fiber can be functionalized and used as the multifunctional template for AuNMT preparation via the same procedure that is used in this study, it is easy to obtain AuNMTs with a length on the order of meters. Also, as an interesting feature, there are many double tubes (Figure 6a) and fork-siamesed tubes (Figure 6b) because of the random arrangement of the neighboring fibers in the nonwoven fabric,

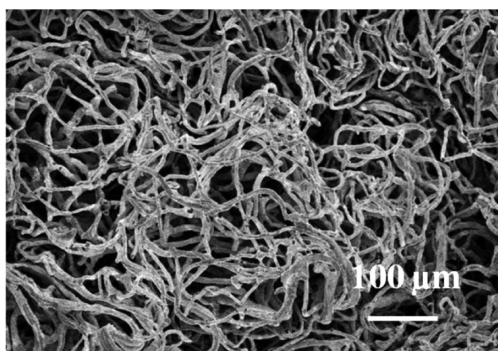


Figure 5. SEM images of the network structure of AuNMTs.

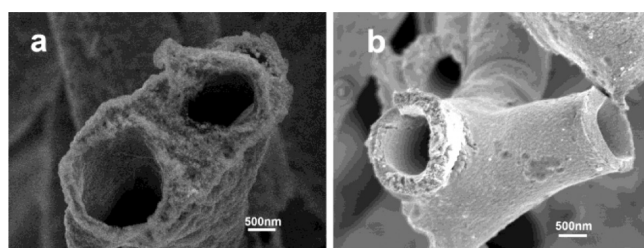


Figure 6. SEM images of the network structure of AuNMTs. SEM images of AuNMTs in the form of (a) double tubes and (b) fork-siamesed tubes.

which can be applied in a future design of an AuNMT network structure.

## CONCLUSIONS

In conclusion, AuNMTs were obtained using a tertiary amine group-functionalized PE/PP nonwoven fabric as a ligand, a reductant, and a template. The polymeric precursor was prepared by radiation-induced graft polymerization of HB onto a PE/PP nonwoven fabric and then reacted with DEA. Because of the different radiation effects of PE and PP, graft polymerization occurs only in the PE shell layer; therefore, the Au(III) ions are absorbed and reduced only in the PE layer, yielding aggregation of AuNPs. Thus, after the calcination, AuNMTs were obtained, and the wall thickness and diameter were determined by the initial Au(III) ion concentration. The shortest wall thickness and diameter obtained were 280 nm and 2.3  $\mu\text{m}$ , respectively, with an initial Au(III) concentration of 1 ppm. The obtained AuNMTs were in a network form, and the length between the junctions is  $\sim 200 \mu\text{m}$ . Along the same lines as this novel approach, it is easy to prepare AuNMTs with a controlled wall thickness and unlimited length using long functionalized fibers, or a complex structure with a designed pattern.

## ASSOCIATED CONTENT

### Supporting Information

SEM image of the pristine PE/PP nonwoven fabric and the PE/PP-g-PHB fabric and TEM image and high-resolution TEM image of the AuNPs on the edge of the AuNMTs after calcination. This material is available free of charge via the Internet at <http://pubs.acs.org>.

## AUTHOR INFORMATION

### Corresponding Author

\*E-mail: [jingyeli@sinap.ac.cn](mailto:jingyeli@sinap.ac.cn).

## Notes

The authors declare no competing financial interest.

## ACKNOWLEDGMENTS

This work was supported by the National Natural Science Foundation of China (Grants 11175234 and 11105210), the “Strategic Priority Research Program” of the Chinese Academy of Sciences (Grant XDA02040300), the “Knowledge Innovation Program” of the Chinese Academy of Sciences (Grant KJCX2-YW-N49), and the Shanghai Municipal Commission for Science and Technology (Grants 11ZR1445400 and 12ZR1453300). H.M. and J.L. thank Mr. Chenyang Xing and Prof. Yongjin Li of Hangzhou Normal University for their help with SEM characterization.

## REFERENCES

- (1) Daniel, M.-C.; Astruc, D. *Chem. Rev.* **2004**, *104*, 293–346.
- (2) Yu, Y.; Kant, K.; Shapter, J. G.; Addai-Mensah, J.; Losic, D. *Microporous Mesoporous Mater.* **2012**, *153*, 131–136.
- (3) Sanchez-Castillo, M. A.; Couto, C.; Kim, W. B.; Dumesic, J. A. *Angew. Chem., Int. Ed.* **2004**, *43*, 1140–1142.
- (4) Velleman, L.; Bruneel, J.-L.; Guillaume, F.; Losic, D.; Shapter, J. G. *Phys. Chem. Chem. Phys.* **2011**, *13*, 19587–19593.
- (5) Taton, T. A.; Mirkin, C. A.; Letsinger, R. L. *Science* **2000**, *289*, 1757–1760.
- (6) Nicewarner-Peña, S. R.; Freeman, R. G.; Reiss, B. D.; He, L.; Peña, D. J.; Walton, I. D.; Cromer, R.; Keating, C. D.; Natan, M. J. *Science* **2001**, *294*, 137–141.
- (7) Jirage, K. B.; Hulteen, J. C.; Martin, C. R. *Science* **1997**, *278*, 655–658.
- (8) Yu, S.; Lee, S. B.; Martin, C. R. *Anal. Chem.* **2003**, *75*, 1239–1244.
- (9) Chen, S.; Yang, Y. *J. Am. Chem. Soc.* **2002**, *124*, 5280–5281.
- (10) Maier, S. A.; Brongersma, M. L.; Kik, S. M. P. G.; Requicha, A. A. G.; Atwater, H. A. *Adv. Mater.* **2001**, *13*, 1501–1505.
- (11) Sun, S.; Murray, C. B.; Weller, D.; Folks, L.; Moser, A. *Science* **2000**, *287*, 1989–1992.
- (12) Faulk, W. P.; Taylor, G. M. *Immunochemistry* **1971**, *8*, 1081–1083.
- (13) Mililigan, W. O.; Morriss, R. H. *J. Am. Chem. Soc.* **1964**, *86*, 3461–3467.
- (14) Sun, Y.; Xia, Y. *Science* **2002**, *298*, 2176–2179.
- (15) Devan, R. S.; Patil, R. A.; Lin, J.-H.; Ma, Y.-R. *Adv. Funct. Mater.* **2012**, *22*, 3326–3370.
- (16) Iijima, S. *Nature* **1991**, *354*, 56–58.
- (17) Wang, J.; Li, Y. *Adv. Mater.* **2003**, *15*, 445–447.
- (18) Jiang, L.; Feng, X. J.; Zhai, J.; Jin, M. H.; Song, Y. L.; Zhu, D. B. *J. Nanosci. Nanotechnol.* **2006**, *6*, 1830–1832.
- (19) Chen, C.-L.; Rosi, N. L. *Angew. Chem., Int. Ed.* **2010**, *49*, 1924–1942.
- (20) Jiang, K.; Eitan, A.; Schädler, L. S.; Ajayan, P. M.; Seigel, R. W.; Grobert, N.; Mayne, M.; Reyes, M. R.; Terrones, H.; Terrones, M. *Nano Lett.* **2003**, *3*, 275–277.
- (21) Dong, W.; Dong, H.; Wang, Z.; Zhan, P.; Yu, Z.; Zhao, X.; Zhu, Y.; Ming, N. *Adv. Mater.* **2006**, *18*, 755–759.
- (22) Shin, T.-Y.; Yoo, S.-H.; Park, S. *Chem. Mater.* **2008**, *20*, 5682–5686.
- (23) Sun, Y. G.; Wiley, B.; Li, Z. Y.; Xia, Y. N. *J. Am. Chem. Soc.* **2004**, *126*, 9399–9406.
- (24) Brumlik, C. J.; Martin, C. R. *J. Am. Chem. Soc.* **1991**, *113*, 3174–3175.
- (25) Rao, C. N. R.; Govindaraj, A. *Adv. Mater.* **2009**, *21*, 4208–4233.
- (26) Martin, C. R.; Nishizawa, M.; Jirage, K.; Kang, M. *J. Phys. Chem. B* **2001**, *105*, 1925–1934.
- (27) Calvar, M. S.; Pacifico, J.; Juste, J. P.; Liz-Marzan, L. M. *Langmuir* **2008**, *24*, 9675–9681.
- (28) Sun, Y.; Xia, Y. *Adv. Mater.* **2004**, *16*, 264–268.

- (29) Zhao, Y.; Jiang, L. *Adv. Mater.* **2009**, *21*, 3621–3638.
- (30) Wang, H. W.; Sheih, C. F.; Chen, H. Y.; Shiu, W. C.; Russo, B.; Cao, G. *Nanotechnology* **2006**, *17*, 2689–2469.
- (31) Ochanda, F.; Jones, W. E. *Langmuir* **2005**, *21*, 10791–10796.
- (32) He, H.; Cai, W.; Lin, Y.; Dai, Z. *Langmuir* **2011**, *27*, 1551–1555.
- (33) Han, C. C.; Bai, M. Y.; Lee, J. T. *Chem. Mater.* **2001**, *13*, 4260–4268.
- (34) Little, B. K.; Li, Y.; Cammarata, V.; Broughton, R.; Mills, G. *ACS Appl. Mater. Interfaces* **2011**, *3*, 1965–1973.
- (35) Makuuchi, K.; Cheng, S. *Radiation Processing of Polymer Materials and Its Industrial Applications*; John Wiley & Sons, Inc.: Hoboken, NJ, 2012.
- (36) Seko, N.; Tamada, M.; Yoshii, F. *Nucl. Instrum. Methods Phys. Res., Sect. B* **2005**, *236*, 21–29.
- (37) Deng, B.; Cai, R.; Yu, Y.; Jiang, H. Q.; Wang, C. L.; Li, J.; Li, L. F.; Yu, M.; Li, J. Y.; Xie, L. D.; Huang, Q.; Fan, C. H. *Adv. Mater.* **2010**, *22*, 5473–5477.
- (38) Yu, M.; Wang, Z. Q.; Liu, H. Z.; Xie, S. Y.; Wu, J. X.; Jiang, H. Q.; Zhang, J. Y.; Li, L. F.; Li, J. Y. *ACS Appl. Mater. Interfaces* **2013**, *5*, 3697–3703.
- (39) Seko, N.; Bang, L. T.; Tamada, M. *Nucl. Instrum. Methods Phys. Res., Sect. B* **2007**, *265*, 146–149.
- (40) Parajuli, D.; Hirota, K.; Inoue, K. *Ind. Eng. Chem. Res.* **2009**, *48*, 10163–10168.
- (41) Feng, C.; Gu, L.; Yang, D.; Hu, J.; Lu, G.; Huang, X. *Polymer* **2009**, *50*, 3990–3996.